

Dalton Transactions

Accepted Manuscript



This is an *Accepted Manuscript*, which has been through the Royal Society of Chemistry peer review process and has been accepted for publication.

Accepted Manuscripts are published online shortly after acceptance, before technical editing, formatting and proof reading. Using this free service, authors can make their results available to the community, in citable form, before we publish the edited article. We will replace this *Accepted Manuscript* with the edited and formatted *Advance Article* as soon as it is available.

You can find more information about *Accepted Manuscripts* in the [Information for Authors](#).

Please note that technical editing may introduce minor changes to the text and/or graphics, which may alter content. The journal's standard [Terms & Conditions](#) and the [Ethical guidelines](#) still apply. In no event shall the Royal Society of Chemistry be held responsible for any errors or omissions in this *Accepted Manuscript* or any consequences arising from the use of any information it contains.

**Diving into the redox properties of *Geobacter sulfurreducens* cytochromes:
a model for extracellular electron transfer**

Telma C. Santos, Marta A. Silva, Leonor Morgado, Joana M. Dantas and Carlos A.
Salgueiro *

UCIBIO, REQUIMTE, Departamento de Química, Faculdade de Ciências e Tecnologia,
Universidade Nova de Lisboa, 2829-516 Caparica, Portugal

* *Corresponding author*: csalgueiro@fct.unl.pt

Abstract

Geobacter bacteria have a remarkable respiratory versatility that includes the dissimilatory reduction of insoluble metal oxides in natural habitats and electron transfer to electrode surfaces from which electricity can be harvested. In both cases, electrons need to be exported from cell interior to outside *via* a mechanism designated extracellular electron transfer (EET). Several *c*-type cytochromes from *G. sulfurreducens* (*Gs*) were identified as key players in this process. Biochemical and biophysical data have been obtained for ten *Gs* cytochromes, including inner-membrane associated (MacA), periplasmic (PpcA, PpcB, PpcC, PpcD, PpcE and GSU1996) and outer membrane associated (OmcF, OmcS and OmcZ). The redox properties of these cytochromes have been determined, except for PpcC and GSU1996. In this perspective, the reduction potentials of these two cytochromes were determined by potentiometric redox titrations followed by visible spectroscopy. The data obtained are taken together with those available for other key cytochromes to present a thorough overview of the current knowledge of *Gs* EET mechanisms and provide a possible rationalization for the existence of several multiheme cytochromes involved in the same respiratory pathways.

Introduction

Dissimilatory metal reducing bacteria (DMRB) can transfer electrons to insoluble metallic compounds in natural habitats and to the surface of terminal acceptors outside the cell to support their respiratory metabolism, in a process designated extracellular electron transfer (EET)¹. The DMRB gained notoriety from the time when it was realized that they represent excellent targets for bioremediation of contaminated sediments, soils and ground waters^{2,3} and, more recently, as current producers in microbial fuel cells^{4,5}. Bacteria from the genus *Shewanella* and *Geobacter* have been the focus for EET studies (for a review see⁶). Understanding EET mechanisms is crucial to develop and improve DMRB-based biotechnological applications, a task that requires the identification of relevant proteins and the characterization of their functional mechanisms. The bacteria *S. oneidensis* MR-1 (*So*) and *G. sulfurreducens* (*Gs*) have been used as model organisms to study EET, since they were the first species with complete genomes sequenced and genetic systems established⁷⁻⁹. Both genomes contain numerous genes encoding for *c*-type cytochromes (42 for *So* and 111 for *Gs*)^{8,9}.

To date, the EET pathways of *So* are better described compared to those of *Gs*. In the first microorganism, the inner membrane (IM) associated tetraheme cytochrome CymA receives electrons from the menaquinone pool and acts as a redox hub, distributing electrons to various cytochromes at periplasmic space^{10,11}. At this point, the small tetraheme cytochrome *c* and the flavocytochrome *c*₃ transfer electrons to the decaheme cytochrome MtrA, the periplasmic component of the MtrA-MtrB-MtrC complex associated with the outer membrane (OM)¹². It has been demonstrated that the extracellular component of this complex (MtrC) interacts with another OM dodecaheme

cytochrome OmcA^{13,14} and can act as reductases for external substrates. Alternatively, the small tetraheme cytochrome can also transfer electrons to decaheme cytochromes MtrD and DmsE, which are the periplasmic components of the OM complexes MtrD-MtrE-MtrF and DmsE-DmsF-DmsA, respectively^{15,16}. The detailed discussion of EET pathways in *So* is beyond this perspective and are illustrated in Figure 1 for sake of completeness (for recent reviews see^{12,17,18}).

Gene knockout and proteomic studies led to the identification of several *c*-type cytochromes that are essential for EET pathways also in *Gs*^{8,19-27}. Biochemical and biophysical data, including redox potential measurements, have been obtained for (i) the IM associated cytochrome MacA²⁸, (ii) the periplasmic cytochromes, including the five members of PpcA-family designated (PpcA-PpcE) and the cytochrome GSU1996²⁹⁻³⁴, and (iii) OM associated cytochromes OmcF, OmcS and OmcZ³⁵⁻³⁷. Genetic studies, carried out on *Gs* mutated strains with gene encoding these cytochromes deleted, together with proteomic analysis indicated that the proteins are involved in the extracellular reduction of Fe(III), U(VI), Mn(IV) or in the current production by microbial fuel cells. A summary of the gene knockout and proteomic studies involving these cytochromes is indicated in Table 1. Amongst these protein, no functional information was obtained for PpcC and the data available for GSU1996 was obtained in different experimental conditions³². Therefore, in this perspective, the redox properties of these cytochromes were determined at physiological pH for *Gs* growth (pH 7) by potentiometric redox titrations followed by visible spectroscopy. The results obtained, allowed us to complete the information on the functional working potential ranges for this group of ten cytochromes and is taken together to suggest a functional model for EET in *Gs*.

Structural and functional features of *G. sulfurreducens* cytochromes involved in extracellular electron transfer

Although several cytochromes essential for EET in *Geobacter* have been identified, the electron transport from cellular interior to exterior in a bioenergetic point of view remains unclear. In this perspective we aimed to contribute to this elucidation by reviewing and complementing the data available for IM, periplasmic and OM *Gs* cytochromes involved in EET. Previous studies provided insights on the redox properties of IM cytochrome MacA, periplasmic cytochromes (PpcA, PpcB, PpcD, PpcE and GSU1996) and OM cytochromes OmcS, OmcZ and OmcF^{28,32,34-37}. Their structures (except for OmcS and OmcZ) have been also determined²⁸⁻³⁷. The structures showed that the redox center(s) of the cytochromes have different degrees of organization. The cytochrome MacA contains 325 residues (36.3 kDa) and two low-spin heme groups axially coordinated by two histidine residues (His-His). On the other hand, the members of the periplasmic PpcA-family are smaller proteins with approximately 10 kDa and contain three low-spin heme groups with His-His axial coordination³⁰. The dodecaheme cytochrome GSU1996 (42.3 kDa) is composed by four similar triheme domains, designated A, B, C and D, connected by a flexible linker, where in each domain there is a co-existence of low-spin hemes containing both His-His and His-Met axial coordination. Within each domain two hemes have His-His axial coordination, whereas the third one is axially coordinated by one histidine and one methionine residue (His-Met)³². The iron-to-iron distance between the closest pairs of heme in each domain (11.2 to 12.1 Å) is similar to the ones observed for triheme periplasmic cytochromes (see Fig. 2).

The OM cytochromes OmcS, OmcZ and OmcF also show considerable variability in their number of redox centers. Cytochrome OmcF is monohemic, whereas OmcS and OmcZ contain 6 and 8 heme groups, respectively. The heme group of cytochrome OmcF is low-spin and has His-Met axial coordination. The structures of OmcS and OmcZ are not yet available and their number of hemes was determined by pyridine hemochrome assays^{35,36}. Details about the spin-state and axial coordination of the hemes in OmcS and OmcZ were obtained from the analysis of their spectroscopic features in solution, which suggested that they are low-spin and axially coordinated by two histidine residues^{35,36}.

As a consequence of the diversity in the number of redox centers in this group of ten cytochromes, different levels of information were obtained from their redox characterization. In case of monoheme cytochrome OmcF, the E_{app} value (*i.e.*, the point at which the oxidized and reduced fractions are equal) corresponds to the reduction potential of the heme group (Supplementary Fig. S1 A). On the other hand, the presence of several hemes makes the detailed thermodynamic characterization of multiheme cytochromes quite complex. In this case several microstates can co-exist in solution connecting the fully reduced and fully oxidized states (for a review see³⁸). These microstates can be grouped according to the number of oxidized hemes in macroscopic oxidation stages linked by successive one-electron reductions (Supplementary Fig. S1 B and C). Therefore, the potentiometric redox titration curves obtained for multiheme cytochromes do not provide sufficient independent pieces of information to discriminate each heme reduction potential, and consequently only describe the macroscopic redox behaviour of the proteins^{35-37,39}. Exceptions are observed for multiheme cytochromes containing non-interacting redox centres whose macroscopic reduction potentials differ

considerably (~ 100 mV). Unfortunately this is not the common feature and the presence of spatially closed hemes mutually modulates their reduction potentials *via* heme-heme redox interactions. Therefore, under this scenario to characterize the individual redox centres it is necessary to monitor the oxidation profile of each heme at different pH values by 2D-exchange NMR spectroscopy (EXSY) and complement the NMR information with data obtain from potentiometric redox titrations monitored by visible spectroscopy³⁸. However, the increase in the protein molecular weight and/or number of hemes leads to the decrease of the NMR spectral quality, as a result of signal overlapping, and usually impairs the monitorization of the individual heme oxidation profiles. To date, the detailed thermodynamic characterization of multiheme cytochromes is limited to proteins containing up to four heme groups and 64 kDa molecular weight (for a review see Pessanha and co-workers⁴⁰). Therefore, the redox characterization of larger multiheme proteins can only be accomplished at macroscopic level.

In respect to the *Gs* cytochromes addressed in this perspective, the redox characterization of the monoheme OmcF, di-heme MacA and triheme PpcA-family (PpcA, PpcB, PpcD and PpcE) was obtained at both macroscopic and microscopic level (Table 2). For OmcF the E_{app} value (+180 mV) corresponds to the reduction potential of the heme group³⁷. Also for diheme cytochrome MacA, the determined macroscopic redox potentials (-237 mV and -138 mV²⁸) can be assigned to individual hemes (hemes 1 and 2, respectively) since the separation between them is around 100 mV. Such separation indicates that the full oxidation of one of the hemes is fully accomplished before the oxidation of the second starts, and therefore only three microstates co-exist in solution (see Supplementary Fig S1 B).

Compared to MacA, the iron-to-iron distances observed between the closest pair of hemes in the periplasmic triheme cytochromes are considerable smaller (Fig. 2). This suggests that the redox potentials of the heme groups are modulated by redox interactions. Moreover, the redox titration curves of these cytochromes do not show any inflection around 1/3 and 2/3 protein reduction, which indicate that the reduction potentials of the hemes are not sufficiently separated to be obtained exclusively from the redox curves (for a review see Morgado and co-workers³⁴). However, since the molecular weight of each triheme cytochrome is relatively small (~10 kDa) the detailed thermodynamic characterization of the individual redox centres could be obtained from 2D-EXSY NMR and potentiometric redox titrations³⁴. The only exception was cytochrome PpcC, for which the presence of different conformations in solution impaired such characterization⁴¹. The results obtained for the other four cytochromes of the PpcA-family showed that the heme reduction potentials are negative, different from each other but not sufficiently separated to be obtained exclusively from the redox titration curves.

Potentiometric redox titrations were also carried out for cytochromes GSU1996, OmcS and OmcZ^{32,35,36}. However, as mentioned above, for larger cytochromes the assignment of the reduction potentials to the individual redox centers is not possible with the current available methodologies. Therefore, since the individual redox properties of the hemes cannot be determined for all the *Gs* cytochromes involved in EET pathways, their redox titration curves were used to determine both the E_{app} values and the redox-active potential windows, under similar experimental conditions. A similar analysis was described for electron transfer components involved in EET pathways of *Shewanella oneidensis* by Firer-Sherwood and co-workers⁴².

The potential window refers to the range of redox potentials for which the proteins are redox-active, *i.e.* not fully reduced nor fully oxidized. Since there is no data available for triheme cytochrome PpcC and the redox characterization of dodecaheme cytochrome GSU1996 was previously obtained at different experimental conditions³², the E_{app} values for these cytochromes were determined in the present work from potentiometric anaerobic redox titrations followed by visible spectroscopy at pH 7. The two proteins were heterologously expressed in *Escherichia coli* and purified as previously described^{32,33}. All the experimental details are provided in the electronic supplementary information. The redox titration curves obtained for both cytochromes showed no hysteresis, as the reductive and oxidative curves are superimposable (Fig. 3). This indicates that under the experimental conditions used, the proteins can cycle between the fully reduced and fully oxidized states in a reversible way. The fitting of the curves yielded E_{app} values of -143 mV and -124 mV for PpcC and GSU1996, respectively (Table 2). The E_{app} value of PpcC is slightly lower compared to the other PpcA-family members, but the proteins cover a similar window of potentials (Table 2). For both cytochromes, the shape of the curves deviates significantly from ones that considers redox centers with identical reduction potential values (see dashed lines in Fig. 3). This suggests a non-equivalence of the redox centers, as expected for a multiredox protein with spatial closed redox centers (see Fig. 2). The results obtained from the redox characterization of the other *Gs* cytochromes are also summarized in Table 2. Overall, the E_{app} values span from -220 to +180 mV and are consistent with the axial coordination of the heme groups. In fact, cytochromes with His-His axially coordinated hemes have negative values, whereas a positive value was only observed for OmcF whose heme has

His-Met axial coordination. From the analysis of Table 2 it is also observed that the redox-active potential windows of the cytochromes correlate with their number of hemes. This indicates that the hemes are not redox equivalent and provides a rationalization for the involvement of several multiheme cytochromes in the same electron transfer pathway. The exception to this is observed for dodecaheme cytochrome GSU1996, which has a comparable redox window to triheme PpcA-family cytochromes. This feature can be explained by the particular structural architecture of the redox centres in cytochrome GSU1996. In fact, this cytochrome has a 12 nm long crescent shaped structure with the twelve hemes arranged along a polypeptide to form a “nanowire” of hemes. The protein forms a modular structure composed by four domains connected by a flexible linker with homology to triheme cytochromes. Previous studies shown that the redox titrations curves of the full-length protein GSU1996 and hexaheme fragments AB and CD were superimposable and yielded very similar E_{app} values: -119; -123 and -122 mV, for GSU1996, fragment AB and fragment CD, respectively³². Therefore, the functional and structural similarities observed for the triheme domains of GSU1996 explains the smaller redox potential window when compared to OmcS (6 hemes) and OmcZ (8 hemes) cytochromes. The larger potential working range observed for the latter cytochromes also indicates that the redox potentials of their heme groups are more distinct, compared to cytochrome GSU1996.

Macroscopic redox potential windows of *G. sulfurreducens* cytochromes: a model for extracellular electron transfer

In case of *G. sulfurreducens*, electrons released by oxidation of nutrients at bacterial cytoplasm are transferred through a network of *c*-type cytochromes to reach a terminal electron acceptor that is present in the bacterium's environment. The redox-active potential windows of *Gs* cytochromes are indicated in Fig. 4. Except for OmcF, a clear overlap between the potential windows is observed, indicating that electron transfer between the cytochromes is likely to be thermodynamically favorable. Moreover, the results obtained are compatible with several studies using biofilms on electrodes, which have shown that EET is detectable above potentials of about -200 mV *versus* normal hydrogen electrode⁴³⁻⁴⁵. Therefore, the E_{app} values of the cytochromes and their operating potential windows indicate that the proteins are functionally active to transfer electrons toward extracellular acceptors.

The redox potential window of OmcF covers positive values, while those of periplasmic cytochromes are typically negative and would favor a downhill electron transfer (Fig. 4). However, the positive redox window of OmcF then makes the reduction of low potential extracellular electron acceptors more difficult and might prevent an effective electron flow from periplasm (Fig. 4). In fact, there are several lines of evidences in the literature indicating that OmcF is not directly involved in the reduction of soluble Fe (III), and consequently the precise role of this cytochrome is still under debate⁴⁶. Such studies suggested that OmcF can function as a redox potential sensor, be part of a signaling pathway involving proteolysis or required for the appropriate transcription of other genes coding for OM cytochromes required for EET.

As for OmcF, the precise role of cytochrome MacA is still under debate. Seidel and co-workers²⁸ showed that MacA displays hydrogen peroxide reductase activity. On the hand, the similar expression patterns and mutant phenotypes observed for cytochromes MacA and OmcB (see below) suggest that they may function in the same or similar routes of electron transfer⁴⁷. However, investigation of the expression of OmcB revealed that both *omcB* transcript and protein levels were dramatically reduced in a MacA-deficient *Gs* strain growth on soluble Fe (III)¹⁹. Expression of *omcB* gene in trans enable the MacA-deficient mutant to reduce Fe(III) suggesting that MacA could be crucial for the transcription of *omcB* gene and is not directly involved in the electron transfer to Fe(III). Therefore, in this particular electron transfer pathway, a different entry gate for cytoplasmic electrons *via* a yet unidentified protein cannot be excluded. However, for other extracellular electron acceptors, such as U(VI), MacA might be involved in the electron transfer from the inner membrane to the periplasm²⁰.

The overlapping window of potential observed between MacA, periplasmic and OM cytochromes may provide electron transfer to cell exterior with no apparent thermodynamic barriers. After the clearly downhill electron transfer from NADH (NADH/NAD⁺, -320 mV, pH 7) to menaquinone (MQ)/menaquinol (MQH₂) pool (MQ/MQH₂, -74 mV, pH 7), harnessing electrons from this pool to MacA at the cytoplasmic membrane is slightly thermodynamically unfavorable (Fig. 4). *In vivo* this electron transfer step can be made more favorable by lowering the MQ/MQH₂ potential upon binding to quinol oxidase and/or by the high abundance of periplasmic cytochrome acceptors. Though, once cytoplasmic electrons have been transferred to MacA, the overlapping of the functional working potential ranges between the cytochromes in the

network warrant a smooth thermodynamic downhill electron delivery to the OM cytochromes. Therefore, MacA after receiving electrons from the quinol pool could perform a similar role to that attributed to cytochrome CymA in *S. oneidensis* (Fig. 1), for which reduction by MQ/MQH₂ pool was also observed to be slightly thermodynamically unfavorable⁴². Once reduced, MacA can function as a redox hub distributing electrons to various cytochromes at periplasmic space, which are likely reservoir of electrons destined for the OM components^{22,48}. In fact, electrochemical protein-protein interaction studies provided evidence that free PpcA in solution was reduced by MacA adsorbed on pyrolytic edge plane graphite electrodes, suggesting an interaction between the two cytochromes²⁸. The structural similarities observed between the five members of PpcA-family³³, in particular in the positively charge region in the neighborhood of heme IV, the most likely entry gate for electrons in these cytochromes, suggest that they could interact *via* this region with MacA. As observed for the periplasmic triheme cytochromes, each of the four domains in cytochrome GSU1996, also has one of the hemes placed in a more positively-charged region compared to its neighbors³². Therefore, an electrostatic driven interaction between the GSU1996 domains and MacA is also likely to occur.

The reduction of extracellular electron acceptors by *Gs* requires electron transfer across the outer membrane. Very recently it was proposed that the OM cytochromes OmcB and OmcC are part of two trans-outer membrane porin-cytochrome protein complexes. Both complexes are responsible for transferring electrons across the OM to extracellular electron acceptors, such as Fe(III) citrate and ferrihydrite⁴⁹. This complex is formed by a periplasmic *c*-type cytochrome (OmaB/OmaC with 8 heme binding motifs), a porin-like OM protein (OmbB/OmbC with no hemes) and an OM *c*-type cytochrome

(OmcB/OmcC with 12 heme binding motifs). Also, it was proposed that these proteins are similar to MtrA-MtrB-MtrC complex in *S. oneidensis*⁵⁰ (cf Figs. 1 and 5). As for OmcS and OmcZ, cytochrome OmcE is also an important extracellular electron transfer component in *Gs* respiratory pathways²³. Gene-knockout studies revealed that this cytochrome is involved in the reduction of U(VI)²⁰, Fe(III) citrate⁴⁸ and Mn(IV) oxides²³. Deletion of *omcE* gene had no impact on current production²⁵. Unfortunately, neither the putative trans-outer membrane protein components nor OmcE have been structural or functional characterized. Despite this, OmcS and OmcZ showed large potential windows centered at -212 and -220 mV, respectively (Table 2). OmcZ is found loosely attached to the outer-surface matrix⁵¹, while OmcS has been found to coat pili⁵², conductive proteic filaments proposed to be required for long-range EET for Fe(III) oxides and for high-density current production in microbial fuel cells^{53,54}. Therefore, OmcS and OmcZ would be predicted to be most accessible to the exogenous extracellular acceptors. The broad redox-active windows of OmcS and OmcZ are centered at low reduction potential values but still overlap with those of periplasmic cytochromes (Fig. 4). This apparent counterintuitive arrangement was previously addressed by Liu and co-workers⁴³ while monitoring the cytochrome redox status in living *Gs*. A hypothesis for this arrangement is that cells evolved to guarantee that their outer surface network is always in an oxidized state, so they may always act as an acceptor for the periplasmic cytochrome pool. This hypothesis was also successfully tested in electrochemical simulations of *Geobacter* biofilms⁵⁵. The broad operating potential ranges for these cytochromes make thermodynamically feasible to transfer electron for extracellular acceptors with different

redox potentials providing bacterium adaptability to face slightly modified redox potentials environments.

Conclusions

The analysis of the data provided by the redox characterization of *Gs* cytochromes implicated in EET, suggests an overlap between their redox-active potential ranges to assure a smooth electron flow from the cytoplasmic oxidation of nutrients to terminal electron acceptors at the cell exterior (Fig. 5). The apparent inexistence of notorious downhill electron transfer steps between the electron transfer components could also explain the low cellular yields obtained when extracellular acceptors are used. Moreover, the study described in this perspective suggests that the overlapping between the redox-active potential of electron transfer components might be typical for any particular EET pathway. Indeed, besides the fact that most of the cytochromes under scrutiny are involved in iron and/or uranium oxide reduction pathways they do not share necessarily all the EET pathways, as suggested by genetic and proteomic studies (Table 1). This is the case of cytochrome OmcS whose deleted mutant affected the reduction of manganese oxides²³ and OmcZ that is directly involved in EET to electrodes²⁵.

The isopotential window that allows a smooth electron flow from the cell interior to exterior was also observed for the components involved in EET in *Shewanella oneidensis*⁴², and might constitute the *modus operandi* of dissimilatory metal reducing bacteria for which it may be beneficial to minimize dissipation of free energy across electron transfer networks. Such *modus operandi* also provides an explanation for the large abundance of multiheme *c*-type cytochromes participating in EET in these bacteria.

In fact, the presence of several redox centers in a single protein is advantageous for electron transfer by (i) increasing the reduction power of the cells⁵⁶, (ii) expanding the protein redox-active windows *via* heme-heme interactions between neighboring redox centers^{57,58}, and (iii) facilitating electron transfer across large distances without the need for transient recognition and binding between successive physiological partners. This clearly contrasts with proteins containing a single redox center, which have a range of redox activity limited by the Nernst curve.

Future investigation on the detailed physical organization of *G. sulfurreducens* EET respiratory networks should definitely involve protein-protein interactions studies to survey the redox pairs and hence to provide important mechanistic details.

Acknowledgments

This work was supported by project grant PTDC/BBB-BEP/0753/2012 (to CAS), UID/Multi/04378/2013 (to UCIBIO - REQUIMTE) and the re-equipment grant REEQ/336/BIO/2005 from Fundação para a Ciência e a Tecnologia (FCT), Portugal.

Table 1 Summary of gene knockout and proteomic studies on *G. sulfurreducens* c-type cytochromes for which biochemical and biophysical data, including redox potential measurements, are available. Mac, membrane associated cytochrome; Ppc, periplasmic cytochrome; Omc, outer membrane cytochrome.

Protein	Gene	Gene knockout and proteomic studies
MacA	<i>gsu0466</i>	In the deletion mutant: reduction of Fe(III) and U(VI) are affected ^{19,20} . More abundant during growth with Fe(III) oxides <i>versus</i> Fe(III) citrate as electron acceptor ²¹ .
PpcA	<i>gsu0612</i>	In the deletion mutant: reduction of Fe(III) and U(VI) are affected ^{20,22} . Detected in both Fe(III) citrate and Fe(III) oxide cultures ²¹ .
PpcB	<i>gsu0364</i>	In the double deletion mutant with PpcC: U(VI) reduction is affected ²⁰ . Detected in both Fe(III) citrate and Fe(III) oxide cultures, but more abundant in Fe(III) citrate ²¹ .
PpcC	<i>gsu0365</i>	In the double deletion mutant with PpcB: U(VI) reduction is affected ²⁰ .
PpcD	<i>gsu1024</i>	In the deletion mutant: reduction of U(VI) is affected ²⁰ . More abundant during growth with Fe(III) oxides <i>versus</i> Fe(III) citrate as electron acceptor ²¹ .
PpcE	<i>gsu1760</i>	In the deletion mutant: reduction of U(VI) is affected ²⁰ . Found only in cultures with Fe(III) citrate ²¹ .
GSU1996	<i>gsu1996</i>	More abundant during growth with Fe(III) citrate <i>versus</i> Fe(III) oxide as electron acceptor ²¹ .
OmcF	<i>gsu2432</i>	In the deletion mutant: reduction of Fe(III) and U(VI) are affected ²⁰ . It was also observed a decreased in the current production ²⁴ .
OmcS	<i>gsu2504</i>	In the deletion mutant: growth in Fe(III) and Mn(IV) oxides is affected ²³ ; there is no impact in the current production ²⁵ . More abundant during growth with Fe(III) oxides <i>versus</i> Fe(III) citrate as electron acceptor ²¹ .
OmcZ	<i>gsu2076</i>	In the deletion mutant: current production and biofilm formation is inhibited ²⁵ . More abundant during growth with Fe(III) citrate <i>versus</i> Fe(III) oxides as electron acceptor ²¹ .

Table 2 Data set of *G. sulfurreducens* c-type cytochromes participating in extracellular electron transfer pathways. ‘IM’ stands for inner membrane, ‘OM’ for outer membrane, ‘P’ for periplasmic, E_{app} for the midpoint reduction potential correspondent to the point at which the oxidized and reduced fractions are equal, and ‘NHE’ for normal hydrogen electrode.

Protein	Predicted localization	Number of residues ^a	Molecular weight (kDa) ^b	Number of hemes	Heme axial ligands	E_{app} (mV) versus NHE ^d	Potential window (mV)
MacA	IM	325	36.3	2	His-Met	-188 ²⁸	250
GSU1996	P	318	42.3	12	His-His; His-Met	-124 (this work)	320
PpcA		71	9.6	3	His-His	-117 ²⁹	285
PpcB		71	9.6	3	His-His	-137 ²⁹	270
PpcC		75	9.6	3	His-His	-143 (this work)	265
PpcD		72	9.6	3	His-His	-132 ³⁴	275
PpcE		70	9.7	3	His-His	-134 ³⁴	280
OmcZ ^c	OM	259	32.7	8	Not determined	-220 ³⁵	405
OmcF		104	11.0	1	His-Met	+180 ³⁷	240
OmcS		409	46.8	6	His-His	-212 ³⁶	320

^a For each protein the total number of residues do not include the signal peptide sequence.

^b The total molecular weight were determined from the total number of residues plus the molecular mass corresponding the heme group(s) (616.5 Da per heme)

^c OmcZ is present in large (OmcZ_L = 50 kDa) and small (OmcZ_s = 30 kDa) forms. The data presented refer to OmcZ_s, which is the predominant extracellular form of OmcZ and retains the eight heme groups.

^d The potential window were determined from potentiometric redox curves considering 1-99% range for protein reduction/oxidation.

FIGURE LEGENDS

Fig. 1 Proposed model for extracellular electron transfer in *Shewanella oneidensis*^{12,17,18}. The oxidation of organic molecules releases electrons to menaquinone (MQ) pool *via* NADH dehydrogenase. From this point, a network of *c*-type cytochromes is responsible for the long-range electron transfer from MQH₂ pool to extracellular acceptors. CymA is proposed to accept electrons from MQH₂ pool, which are then delivered to multiheme periplasmic cytochromes, which establish the interface between the cytoplasmic and OM associated electron transfer components. The arrows indicate the proposed flow for electrons. Solid arrows connecting periplasmic components indicate the pairwise interactions identified by NMR experiments¹². The structures of cytochromes from *S. oneidensis* were drawn using the PyMOL molecular graphics system: STC (PDB 1M1Q⁵⁹); FccA (PDB 1D4D⁶⁰); MtrF (PDB 3PMQ⁶¹); OmcA (PDB 4LMH⁶²). Cartoons illustrate electron transfer components for which no structures are available: (i) OM complexes MtrA-MtrB-MtrC, MtrD-MtrE-MtrF and DmsE-DmsF-DmsA (ii) cytochrome CymA and (iii) NADH dehydrogenase. The heme groups in these cytochromes are represented by white circles. For recent reviews on *S. oneidensis* EET see^{12,17,18}.

Fig. 2 Spatial arrangement of the redox centres in multiheme cytochromes MacA (PDB 4AAL²⁸), PpcC (PDB 3H33³³) and GSU1996 (PDB 3OV0³²) from *G. sulfurreducens*. Iron-iron distances between the closest heme groups are indicated. The structure of PpcC illustrates the conserved heme core arrangement between the PpcA-family periplasmic cytochromes^{29,30,33}.

Fig. 3 Potentiometric redox titrations followed by visible spectroscopy of PpcC and GSU1996 (pH 7). The open and filled symbols represent the data points in the reductive and oxidative direction, respectively. Solid lines indicate the result of the fits for the model of consecutive reversible redox steps between the different oxidation stages (see Fig. S1). The dashed lines describes the redox curve considering equivalence of the redox centers with the reduction potential of -143 mV and -124 mV for PpcC and GSU1996, respectively. The inset shows the α -band region of the visible spectra used for the redox

titration. The structures of PpcC (PDB 3H33³³) and GSU1996 (PDB 3OV0³²) were generated in PyMOL molecular graphics system.

Fig. 4 Histogram comparison of the redox-active windows of *G. sulfurreducens* cytochromes at pH 7. Horizontal black lines correspond to the reduction potential of the hemes: MacA (-237 and -138 mV²⁸); PpcA (-147, -104, -111 mV, for hemes I, III and IV, respectively); PpcB (-146, -156, -119 mV); PpcD (-150, -96, -151 mV) and PpcE (-154, -161, -96 mV). The reduction potential values for the PpcA-family heme groups were calculated from their thermodynamic parameters determined for fully reduced and protonated proteins³⁴. The spatial arrangement of the hemes in triheme cytochromes is superimposable with that of the structurally homologous tetraheme cytochromes *c*₃, with the sole difference in the absence of the haem II and the correspondent polypeptide segment. For this reason, the heme groups are numbered I, III, and IV. For the sake of completeness the reduction potential values for NADH/NAD⁺ (-320 mV), MQ/MQH₂ (-74 mV) and typical extracellular electron acceptors are also included. The dashed rectangle corresponds to the potential range exhibited by the most abundant iron oxides from natural environments such as goethite, magnetite, or ferrihydrite (-310 to +10 mV versus NHE)⁶³.

Fig. 5 Proposed model for extracellular electron transfer in *G. sulfurreducens*. The oxidation of organic molecules releases electrons to menaquinone (MQ) pool via NADH dehydrogenase. From this point, a network of *c*-type cytochromes is responsible for the electron transfer from MQH₂ pool to extracellular acceptor. MacA is proposed to accept electrons from MQH₂ pool, which are delivered to multiheme periplasmic cytochromes, which then assure electron transfer between cytoplasmic and OM electron transfer components. The arrows indicate the proposed flow for electrons. The structures of cytochromes from *G. sulfurreducens* were drawn using the PyMOL molecular graphics system: MacA (PDB 4AAL²⁸); PpcA (PDB 2LDO³⁰); PpcB (PDB 3BXU²⁹); PpcC (PDB 3H33³³); PpcD (PDB 3H4N³³); PpcE (PDB 3H34³³); GSU1996 (PDB 3OV0³²); OmcF (PDB 3CU4³⁷) and PilA (PDB 2M7G⁶⁴). Cartoons illustrate electron transfer components for which no structures are available: (i) OM porin:cytochrome complex OmaB/OmaC;

OmbB/OmbC and OmcB/OmcC; (ii) cytochromes OmcZ and OmcS; (iii) NADH dehydrogenase; (iv). The heme groups in OmcZ and OmcS are represented by white circles.

References

1. D. R. Lovley, *Annu. Rev. Microbiol.*, 1993, **47**, 263.
2. K. H. Nealson, A. Belz and B. McKee, *Antonie Van Leeuwenhoek*, 2002, **81**, 215.
3. D. R. Lovley, *Science*, 2001, **293**, 1444.
4. D. R. Lovley, *Nat. Rev. Microbiol.*, 2006, **4**, 497.
5. H. H. Hau and J. A. Gralnick, *Annu. Rev. Microbiol.*, 2007, **61**, 237.
6. K. A. Weber, L. A. Achenbach and J. D. Coates, *Nat. Rev. Microbiol.*, 2006, **4**, 752.
7. M. V. Coppi, C. Leang, S. J. Sandler and D. R. Lovley, *Appl. Environ. Microbiol.*, 2001, **67**, 3180.
8. B. A. Methé, K. E. Nelson, J. A. Eisen, I. T. Paulsen, W. Nelson, J. F. Heidelberg, D. Wu, M. Wu, N. Ward, M. J. Beanan, R. J. Dodson, R. Madupu, L. M. Brinkac, S. C. Daugherty, R. T. DeBoy, A. S. Durkin, M. Gwinn, J. F. Kolonay, S. A. Sullivan, D. H. Haft, J. Selengut, T. M. Davidsen, N. Zafar, O. White, B. Tran, C. Romero, H. A. Forberger, J. Weidman, H. Khouri, T. V. Feldblyum, T. R. Utterback, S. E. Van Aken, D. R. Lovley and C. M. Fraser, *Science*, 2003, **302**, 1967.
9. J. F. Heidelberg, I. T. Paulsen, K. E. Nelson, E. J. Gaidos, W. C. Nelson, T. D. Read, J. A. Eisen, R. Seshadri, N. Ward, B. Methe, R. A. Clayton, T. Meyer, A. Tsapin, J. Scott, M. Beanan, L. Brinkac, S. Daugherty, R. T. DeBoy, R. J. Dodson, A. S. Durkin, D. H. Haft, J. F. Kolonay, R. Madupu, J. D. Peterson, L. A. Umayam, O. White, A. M. Wolf, J. Vamathevan, J. Weidman, M. Impraim, K. Lee, K. Berry, C. Lee, J. Mueller, H. Khouri, J. Gill, T. R. Utterback, L. A. McDonald, T. V. Feldblyum, H. O. Smith, J. C. Venter, K. H. Nealson and C. M. Fraser, *Nat. Biotechnol.*, 2002, **20**, 1118.
10. J. M. Myers and C. R. Myers, *J. Bacteriol.*, 2000, **182**, 67.
11. C. R. Myers and J. M. Myers, *J. Bacteriol.*, 1997, **179**, 1143.
12. B. M. Fonseca, C. M. Paquete, S. E. Neto, I. Pacheco, C. M. Soares and R. O. Louro, *Biochem. J.*, 2013, **449**, 101.
13. H. Zhang, X. Tang, G. R. Munske, N. Zakharova, L. Yang, C. Zheng, M. A. Wolff, N. Tolic, G. A. Anderson, L. Shi, M. J. Marshall, J. K. Fredrickson and J. E. Bruce, *J. Proteome. Res.*, 2008, **7**, 1712.
14. L. Shi, B. Chen, Z. Wang, D. A. Elias, M. U. Mayer, Y. A. Gorby, S. Ni, B. H. Lower, D. W. Kennedy, D. S. Wunschel, H. M. Mottaz, M. J. Marshall, E. A. Hill, A. S. Beliaev, J. M. Zachara, J. K. Fredrickson and T. C. Squier, *J. Bacteriol.*, 2006, **188**, 4705.
15. K. E. Pitts, P. S. Dobbin, F. Reyes-Ramirez, A. J. Thomson, D. J. Richardson and H. E. Seward, *J. Biol. Chem.*, 2003, **278**, 27758.
16. D. Coursolle, D. B. Baron, D. R. Bond and J. A. Gralnick, *J. Bacteriol.*, 2010, **192**, 467.
17. M. Breuer, K. M. Rosso, J. Blumberger and J. N. Butt, *J. R. Soc. Interface.*, 2015, **12**, 1.
18. C. M. Paquete and R. O. Louro, *Dalton Trans.*, 2010, **39**, 4259.

19. B. C. Kim and D. R. Lovley, *FEMS Microbiol. Lett.*, 2008, **39**.
20. E. S. Shelobolina, M. V. Coppi, A. A. Korenevsky, L. N. Didonato, S. A. Sullivan, H. Konishi, H. Xu, C. Leang, J. E. Butler, B. C. Kim and D. R. Lovley, *BMC Microbiol.*, 2007, **7**, 16.
21. Y. H. Ding, K. K. Hixson, M. A. Aklujkar, M. S. Lipton, R. D. Smith, D. R. Lovley and T. Mester, *Biochim. Biophys. Acta.*, 2008, **1784**, 1935.
22. J. R. Lloyd, C. Leang, A. L. Hodges Myerson, M. V. Coppi, S. Cuifo, B. Methe, S. J. Sandler and D. R. Lovley, *Biochem. J.*, 2003, **369**, 153.
23. T. Mehta, M. V. Coppi, S. E. Childers and D. R. Lovley, *Appl. Environ. Microbiol.*, 2005, **71**, 8634.
24. B. C. Kim, B. L. Postier, R. J. Didonato, S. K. Chaudhuri, K. P. Nevin and D. R. Lovley, *Bioelectrochemistry*, 2008, **73**, 70.
25. K. P. Nevin, B. C. Kim, R. H. Glaven, J. P. Johnson, T. L. Woodard, B. A. Methe, R. J. Didonato, S. F. Covalla, A. E. Franks, A. Liu and D. R. Lovley, *PLoS One*, 2009, **4**, e5628.
26. D. E. Holmes, S. K. Chaudhuri, K. P. Nevin, T. Mehta, B. A. Methé, A. Liu, J. E. Ward, T. L. Woodard, J. Webster and D. R. Lovley, *Environ. Microbiol.*, 2006, **8**, 1805.
27. C. Leang, M. V. Coppi and D. R. Lovley, *J. Bacteriol.*, 2003, **185**, 2096.
28. J. Seidel, M. Hoffmann, K. E. Ellis, A. Seidel, T. Spatzal, S. Gerhardt, S. J. Elliott and O. Einsle, *Biochemistry*, 2012, **51**, 2747.
29. L. Morgado, M. Bruix, V. Orshonsky, Y. Y. Londer, N. E. Duke, X. Yang, P. R. Pokkuluri, M. Schiffer and C. A. Salgueiro, *Biochim. Biophys. Acta*, 2008, **1777**, 1157.
30. L. Morgado, V. B. Paixão, M. Schiffer, P. R. Pokkuluri, M. Bruix and C. A. Salgueiro, *Biochem. J.*, 2012, **441**, 179.
31. P. R. Pokkuluri, Y. Y. Londer, N. E. Duke, W. C. Long and M. Schiffer, *Biochemistry*, 2004, **43**, 849.
32. P. R. Pokkuluri, Y. Y. Londer, N. E. Duke, M. Pessanha, X. Yang, V. Orshonsky, L. Orshonsky, J. Erickson, Y. Zagyansky, C. A. Salgueiro and M. Schiffer, *J. Struct. Biol.*, 2011, **174**, 223.
33. P. R. Pokkuluri, Y. Y. Londer, X. Yang, N. E. Duke, J. Erickson, V. Orshonsky, G. Johnson and M. Schiffer, *Biochim. Biophys. Acta*, 2010, **1797**, 222.
34. L. Morgado, M. Bruix, M. Pessanha, Y. Y. Londer and C. A. Salgueiro, *Biophys. J.*, 2010, **99**, 293.
35. K. Inoue, X. Qian, L. Morgado, B. C. Kim, T. Mester, M. Izallalen, C. A. Salgueiro and D. R. Lovley, *Appl. Environ. Microbiol.*, 2010, **76**, 3999.
36. X. Qian, T. Mester, L. Morgado, T. Arakawa, M. L. Sharma, K. Inoue, C. Joseph, C. A. Salgueiro, M. J. Maroney and D. R. Lovley, *Biochim. Biophys. Acta*, 2011, **1807**, 404.
37. P. R. Pokkuluri, Y. Y. Londer, S. J. Wood, N. E. Duke, L. Morgado, C. A. Salgueiro and M. Schiffer, *Proteins*, 2009, **74**, 266.
38. D. L. Turner, C. A. Salgueiro, T. Catarino, J. LeGall and A. V. Xavier, *Eur. J. Biochem.*, 1996, **241**, 723.
39. C. A. Salgueiro, *Global J. Biochem.*, 2012, **3**, 5.

40. M. Pessanha, E. L. Rothery, C. S. Miles, G. A. Reid, S. K. Chapman, R. O. Louro, D. L. Turner, C. A. Salgueiro and A. V. Xavier, *Biochim. Biophys. Acta*, 2009, **1787**, 113.
41. L. Morgado, M. Bruix, Y. Y. Londer, P. R. Pokkuluri, M. Schiffer and C. A. Salgueiro, *Biochem. Biophys. Res. Commun.*, 2007, **360**, 194.
42. M. Firer-Sherwood, G. S. Pulcu and S. J. Elliott, *J. Biol. Inorg. Chem.*, 2008, **13**, 849.
43. Y. Liu, H. Kim, R. R. Franklin and D. R. Bond, *ChemPhysChem*, 2011, **12**, 2235.
44. H. Richter, K. P. Nevin, H. Jia, D. A. Lowy, D. R. Lovley and L. M. Tender, *Energy Environ. Sci.*, 2009, **2**, 506.
45. J. T. Babauta, H. D. Nguyen, T. D. Harrington, R. Renslow and H. Beyenal, *Biotechnol. Bioeng.*, 2012, **109**, 2651.
46. B. C. Kim, C. Leang, Y. H. Ding, R. H. Glaven, M. V. Coppi and D. R. Lovley, *J. Bacteriol.*, 2005, **187**, 4505.
47. M. Aklujkar, M. V. Coppi, C. Leang, B. C. Kim, M. A. Chavan, L. A. Perpetua, L. Giloteaux, A. Liu and D. E. Holmes, *Microbiology*, 2013, **159**, 515.
48. Y. H. Ding, K. K. Hixson, C. S. Giometti, A. Stanley, A. Esteve-Núñez, T. Khare, S. L. Tollaksen, W. Zhu, J. N. Adkins, M. S. Lipton, R. D. Smith, T. Mester and D. R. Lovley, *Biochim. Biophys. Acta.*, 2006, **1764**, 1198.
49. Y. Liu, Z. Wang, J. Liu, C. Levar, M. J. Edwards, J. T. Babauta, D. W. Kennedy, Z. Shi, H. Beyenal, D. R. Bond, T. A. Clarke, J. N. Butt, D. J. Richardson, K. M. Rosso, J. M. Zachara, J. K. Fredrickson and L. Shi, *Environ. Microbiol. Rep.*, 2014, **6**, 776.
50. R. S. Hartshorne, C. L. Reardon, D. Ross, J. Nuester, T. A. Clarke, A. J. Gates, P. C. Mills, J. K. Fredrickson, J. M. Zachara, L. Shi, A. S. Beliaev, M. J. Marshall, M. Tien, S. Brantley, J. N. Butt and D. J. Richardson, *Proc. Natl. Acad. Sci. U S A*, 2009, **106**, 22169.
51. K. Inoue, C. Leang, A. E. Franks, T. L. Woodard, K. P. Nevin and D. R. Lovley, *Environ. Microbiol. Rep.*, 2011, **3**, 211.
52. C. Leang, X. Qian, T. Mester and D. R. Lovley, *Appl. Environ. Microbiol.*, 2010, **76**, 4080.
53. G. Reguera, K. D. McCarthy, T. Mehta, J. S. Nicoll, M. T. Tuominen and D. R. Lovley, *Nature*, 2005, **435**, 1098.
54. G. Reguera, K. P. Nevin, J. S. Nicoll, S. F. Covalla, T. L. Woodard and D. R. Lovley, *Appl. Environ. Microbiol.*, 2006, **72**, 7345.
55. S. M. Strycharz, A. P. Malanoski, R. M. Snider, H. Yi, D. R. Lovley and L. M. Tender, *Energy Environ. Sci.*, 2011, **4**, 896.
56. A. Esteve-Núñez, J. Sosnik, P. Visconti and D. R. Lovley, *Environ. Microbiol.*, 2008, **10**, 497.
57. L. Morgado, A. P. Fernandes, Y. Y. Londer, P. R. Pokkuluri, M. Schiffer and C. A. Salgueiro, *Biochem. J.*, 2009, **420**, 485.
58. B. M. Fonseca, C. M. Paquete, C. A. Salgueiro and R. O. Louro, *FEBS Lett.*, 2011, **586**, 504.
59. D. Leys, T. E. Meyer, A. S. Tsapin, K. H. Nealson, M. A. Cusanovich and J. J. Van Beeumen, *J. Biol. Chem.*, 2002, **277**, 35703.

60. D. Leys, A. S. Tsapin, K. H. Neilson, T. E. Meyer, M. A. Cusanovich and J. J. Van Beeumen, *Nat. Struct. Biol.*, 1999, **6**, 1113.
61. T. A. Clarke, M. J. Edwards, A. J. Gates, A. Hall, G. F. White, J. Bradley, C. L. Reardon, L. Shi, A. S. Beliaev, M. J. Marshall, Z. Wang, N. J. Watmough, J. K. Fredrickson, J. M. Zachara, J. N. Butt and D. J. Richardson, *Proc. Natl. Acad. Sci. USA*, 2011, **108**, 9384.
62. M. J. Edwards, N. A. Baiden, A. Johs, S. J. Tomanicek, L. Liang, L. Shi, J. K. Fredrickson, J. M. Zachara, A. J. Gates, J. N. Butt, D. J. Richardson and T. A. Clarke, *FEBS Lett.*, 2014, **588**, 1886.
63. W. Stumm and J. J. Morgan, *Aquatic chemistry: chemical equilibria and rates in natural waters*, Wiley Publication, 3rd edn, 1996.
64. P. N. Reardon and K. T. Mueller, *J. Biol. Chem.*, 2013, **288**, 29260.

FIGURE 1

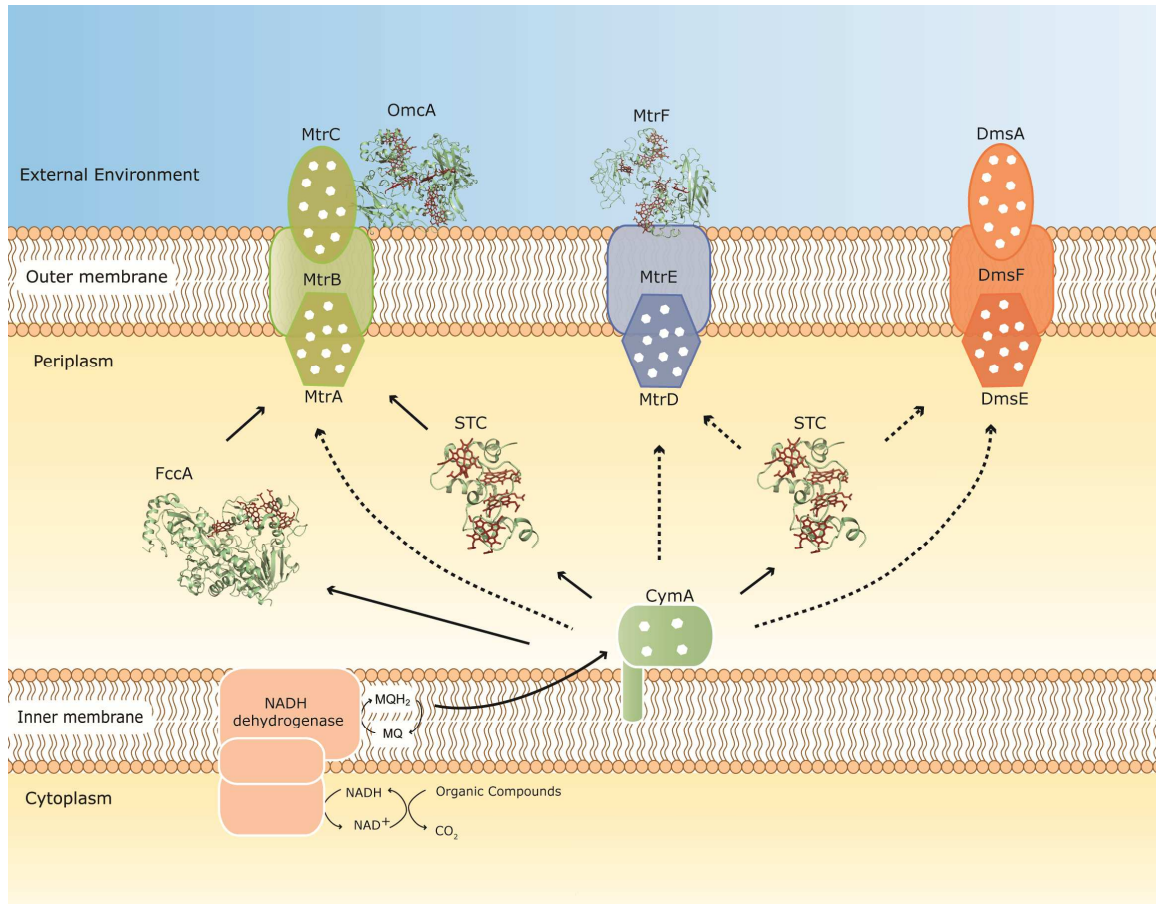


FIGURE 2

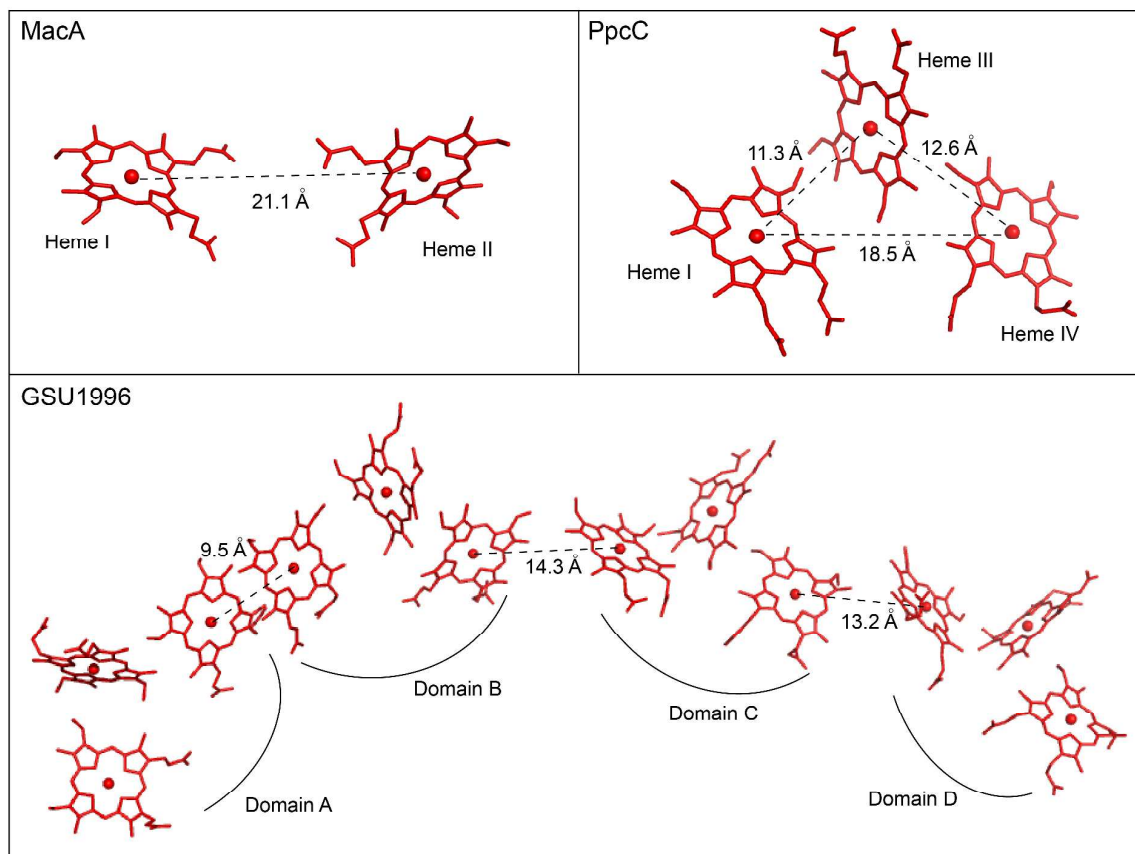


FIGURE 3

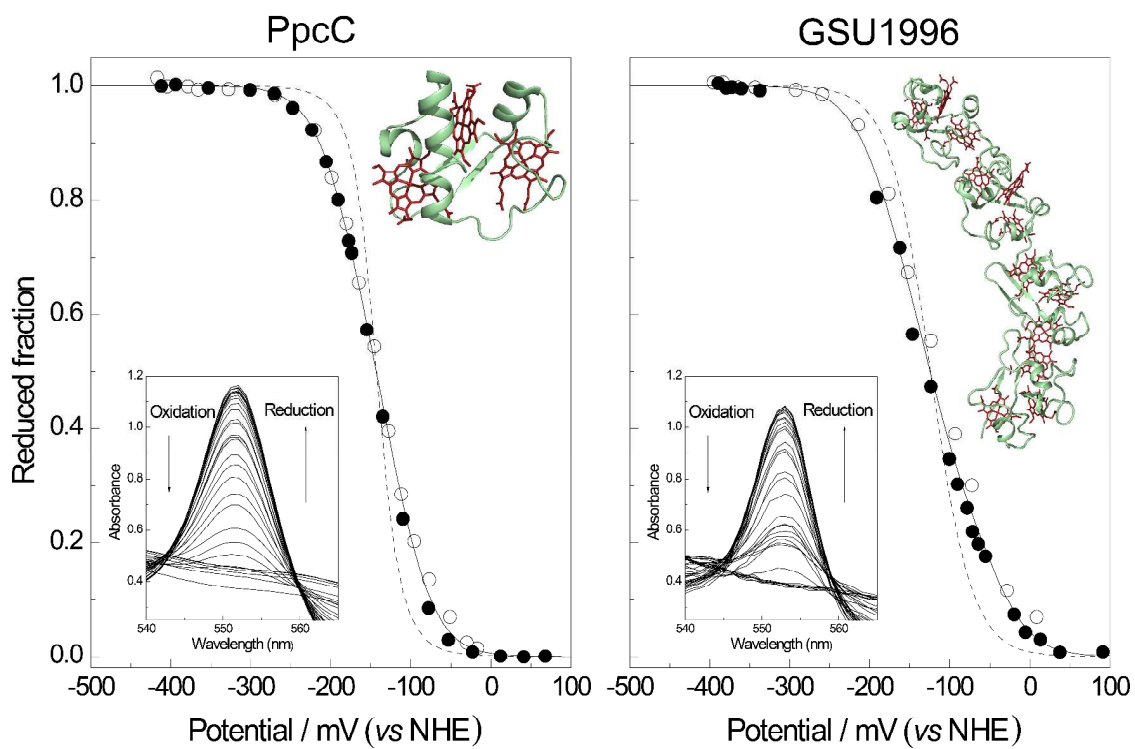


FIGURE 4

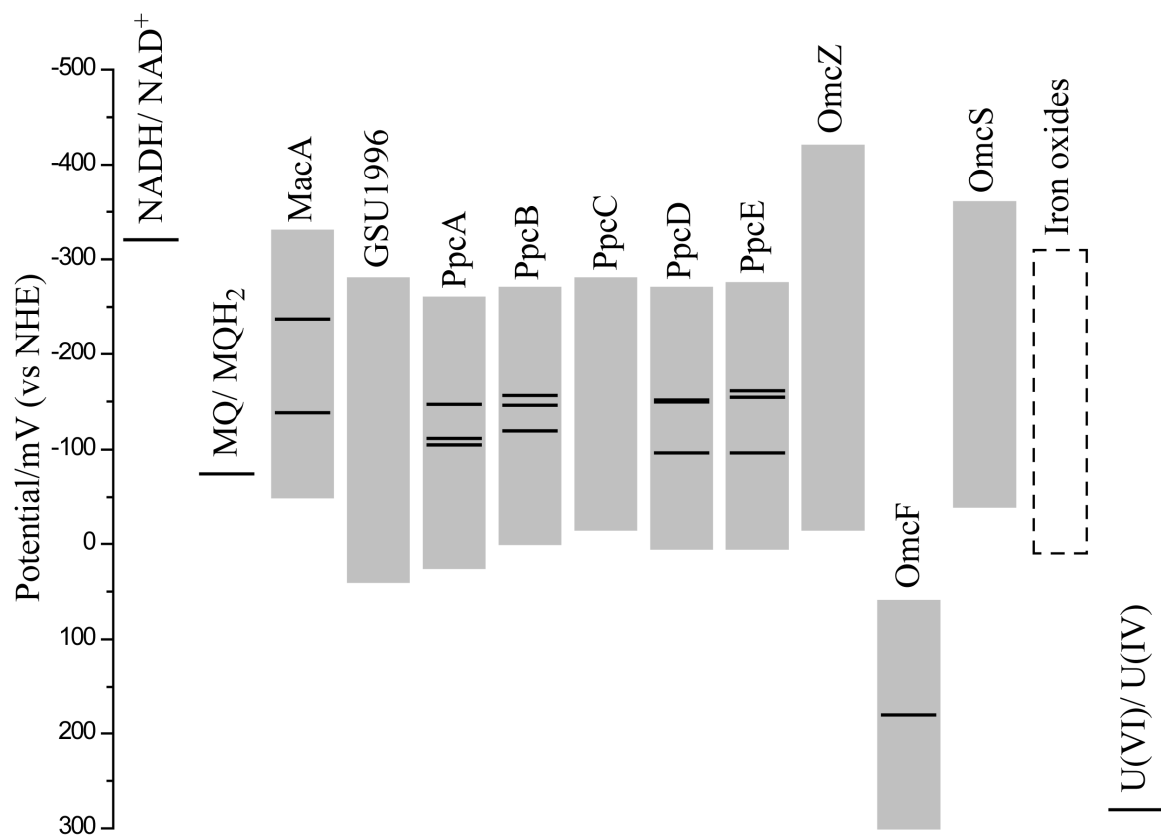


FIGURE 5

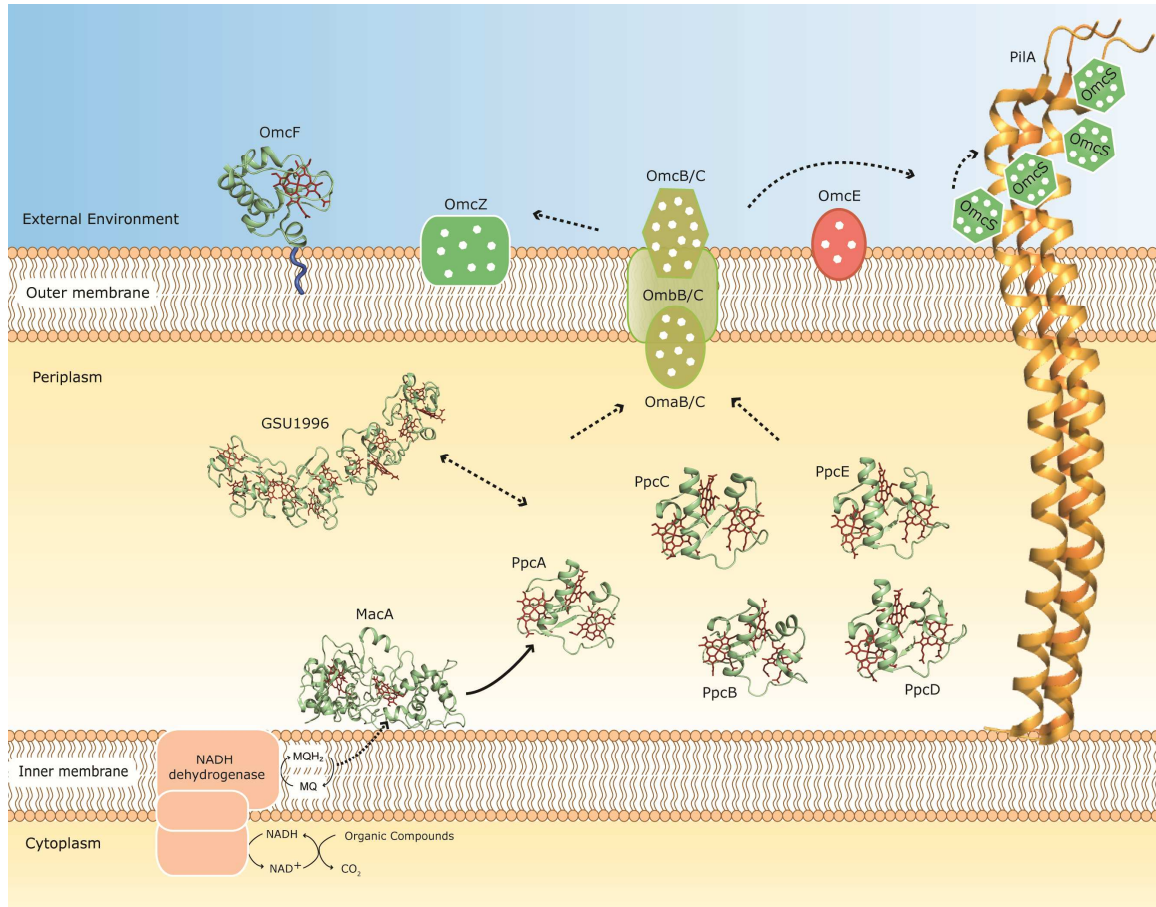


Table of contents

The redox properties of key cytochromes from *Geobacter sulfurreducens* are used to present an overview for extracellular electron transfer pathways

